J Biomol NMR (2013) 55:323–337
DOI 10.1007/s10858-013-9716-z

ARTICLE

# Unraveling a phosphorylation event in a folded protein by NMR spectroscopy: phosphorylation of the Pin1 WW domain by PKA

**Caroline Smet-Nocca · Hélène Launay · Jean-Michel Wieruszeski · Guy Lippens · Isabelle Landrieu**

Received: 9 October 2012 / Accepted: 15 February 2013 / Published online: 2 March 2013
© Springer Science+Business Media Dordrecht 2013

**Abstract** The Pin1 protein plays a critical role in the functional regulation of the hyperphosphorylated neuronal Tau protein in Alzheimer's disease and is by itself regulated by phosphorylation. We have used Nuclear Magnetic Resonance (NMR) spectroscopy to both identify the PKA phosphorylation site in the Pin1 WW domain and investigate the functional consequences of this phosphorylation. Detection and identification of phosphorylation on serine/threonine residues in a globular protein, while mostly occurring in solvent-exposed flexible loops, does not lead to chemical shift changes as obvious as in disordered proteins and hence does not necessarily shift the resonances outside the spectrum of the folded protein. Other complications were encountered to characterize the extent of the phosphorylation, as part of the $^{1}H$,$^{15}N$ amide resonances around the phosphorylation site are specifically broadened in the unphosphorylated state. Despite these obstacles, NMR spectroscopy was an efficient tool to confirm phosphorylation on S16 of the WW domain and to quantify the level of phosphorylation. Based on this analytical characterization, we show that WW phosphorylation on S16 abolishes its binding capacity to a phosphorylated Tau peptide. A reduced conformational heterogeneity and flexibility of the phospho-binding loop upon S16 phosphorylation could account for part of the decreased affinity for its phosphorylated partner. Additionally, a structural model of the phospho-WW obtained by molecular dynamics simulation and energy minimization suggests that the phosphate moiety of phospho-S16 could compete with the phospho-substrate.

**Keywords** NMR spectroscopy · Post-translational modifications · Phosphorylation · Protein · Pin1 WW binding module

**Abbreviations**

| | |
|---|---|
| AD | Alzheimer's disease |
| IDPs | Intrinsically disordered proteins |
| Pin1 | Protein interacting with NIMA-1 |
| NIMA | Never in mitosis gene A |
| PKA | Protein kinase A |
| MALDI-TOF MS | Matrix-assisted laser desorption ionization- time of flight mass spectrometry |
| PTMs | Post translational modifications |
| RP-HPLC | Reverse phase high pressure liquid chromatography |
| WW | Trp–Trp binding module |
| $WW^{PKA}$ | PKA-phosphorylated WW domain |
| Phospho-WW | Phosphorylated form of the WW domain |

**Electronic supplementary material** The online version of this article (doi:10.1007/s10858-013-9716-z) contains supplementary material, which is available to authorized users.

C. Smet-Nocca · H. Launay · J.-M. Wieruszeski · G. Lippens · I. Landrieu
Institut Fédératif de Recherches 147, CNRS UMR 8576, Université de Lille-Nord de France, Villeneuve d'Ascq, France

C. Smet-Nocca (✉)
Unité de Glycobiologie Structurale et Fonctionnelle (CNRS UMR 8576), Université de Lille-Nord de France, Cité Scientifique Bâtiment C9, 59655 Villeneuve d'Ascq, France
e-mail: caroline.smet@univ-lille1.fr

I. Landrieu (✉)
Unité de Glycobiologie Structurale et Fonctionnelle (CNRS UMR 8576), Interdisciplinary Research Institute, Université de Lille-Nord de France, 50 Avenue de Halley, 59658 Villeneuve d'Ascq, France
e-mail: isabelle.landrieu@univ-lille1.fr

## Introduction

Protein phosphorylation is a major regulatory process within eukaryotic cells. Characterization of phosphorylation sites is an important issue to understand the impact of phosphorylation on protein activity and function (Johnson and Barford 1993). To allow phosphorylation-dependent signalling pathways, proteins incorporate modular domains enabling specific recognition of other proteins in their phosphorylated states. The human peptidyl-prolyl *cis/trans* isomerase Pin1 was first implicated in the regulation of cell cycle through interactions with mitotic phospho-proteins by one of these modules, the WW domain (Lu et al. 1996; Yaffe et al. 1997). More recently, functional interactions with phosphorylated neuronal Tau and APP proteins have linked Pin1 to Alzheimer's disease (AD)-neurodegenerative processes (Arosio et al. 2012; Balastik et al. 2007; Bulbarelli et al. 2009; Lonati et al. 2011; Lu et al. 1999; Ma et al. 2012; Pastorino et al. 2006; Sultana et al. 2006). In particular, Tau phosphorylation level regulates its physiological function of microtubule binding and tubulin polymerization as well as the formation of the pathological Tau aggregates, one of the hallmarks of AD. Pin1 was shown to play a critical role in the functional regulation of the hyperphosphorylated neuronal Tau protein in AD neurons as $Pin1^{-/-}$ mice develop an age-related tauopathy (Lu et al. 1999; Liou et al. 2003). For these reasons, molecular characterization of the Pin1 and phospho-Tau interactions has gained attention (Hamdane et al. 2002; Smet et al. 2004, 2005a; b). Interestingly, Pin1 is regulated by phosphorylation itself (Lu et al. 2002; Rangasamy et al. 2012). High levels of phosphorylation of the Pin1 protein are detected in AD affected brain tissues compared to control tissues (Ando et al. 2012). Additionally, phosphorylation of Pin1 was previously shown to affect its cellular function (Lu et al. 2002).

Here, we investigate the phosphorylation by the PKA kinase of the WW domain of Pin1, a small module folded into a triple-stranded β-sheet, localized in the amino-terminal part of the Pin1 protein (Ranganathan et al. 1997; Verdecia et al. 2000; Wintjens et al. 2001). The WW domain of Pin1 exhibits a strong specificity for phosphorylated substrates and is responsible for the binding of phospho-proteins through phospho-S/T–P motifs generated by proline-directed kinases (Yaffe et al. 1997). Phosphorylation of the Pin1 WW domain by PKA was shown to modify the interaction with its partners and leads to a change in sub-cellular localization (Lu et al. 2002). Firstly indirectly identified through experiments involving alanine mutations, the S16 residue located in the phospho-binding loop was proposed to be the phosphorylation site (Lu et al. 2002). Additional evidence comes from the detection of Pin1 hyperphosphorylation at the S16 residue in AD brain tissues when compared with controls (Ando et al. 2012). The investigation of the functional consequences of the Pin1 WW domain phosphorylation required first the analytical characterization of the WW PKA-phosphorylation site(s) in the Nuclear Magnetic Resonance (NMR) sample.

Whereas immunochemistry and mass spectrometry (MS) have been traditionally the methods of choice to detect PTMs (Post-Translational Modifications), both at the level of individual proteins or more largely on a proteome-wide scale, NMR as an analytical technique has recently entered this field (Theillet et al. 2012). Although limited by the requirement of a stable isotope-labeled protein and low sensitivity, its capacity to detect even in a complex mixture a variety of PTMs, its quantitative nature and non-destructive character have all led to propose this biophysical technique as a useful alternative to the above mentioned techniques. In order to increase its general use, we have previously proposed a reference library of the NMR spectral signatures that the various PTMs might cause (Theillet et al. 2012). These signatures can be divided in "*indicators*", spectral characteristics that show that a certain PTM is present in the sample, and "*identifying signals*" that allow the site-specific assignment of the PTM to a given residue. As stated, these spectral signatures are quite generally valid for the PTM of amino acids embedded in intrinsically disordered proteins (IDPs). The "*indicators*" for phosphorylation sites are based on $^{1}H$-$^{15}N$ chemical shift perturbations, while the "*identifying signals*" correspond to the Cα and Cβ chemical shifts of the phospho-S/T residues (Bienkiewicz and Lumb 1999; Theillet et al. 2012). Whereas disordered regions often tend to harbor regulatory PTMs (Iakoucheva et al. 2004), many examples equally exist whereby PTMs are found in the context of globular proteins. Although often located on residues in accessible and flexible loops of proteins, PTMs are embedded in these structured proteins and therefore, their NMR-based detection and characterization do not necessarily obey the same rules as for IDPs. One major issue for the identification of a modification site in a globular protein is to differentiate the chemical shift changes that are related to the secondary or tertiary structural changes from those related to the modification itself. A second issue concerns the determination of the extent of modification as phosphorylation can have an effect on both water exchange and relaxation rates complicating the quantification due to specific line broadening. This effect probably is quite general, as phosphorylation has been shown to be responsible for stabilization/destabilization of local secondary structure (Andrew et al. 2002; Baker et al. 2007; Pufall et al. 2005) and introduction of negative charges through the phosphate moiety will result in water exchange rate perturbations (Bai et al. 1993).

Despite numerous NMR studies that have carefully evaluated the role of phosphorylation on protein structures

and on the modulation of protein–protein interfaces, the modification site is generally not identified by NMR, or at best only assessed by $^{1}$H-$^{15}$N chemical shift mapping (Eto et al. 2007; Ohki et al. 2001; Pullen et al. 1995; Teriete et al. 2009; Wittekind et al. 1989). The analytical characterization of the PKA phosphorylation of the WW domain is thus here addressed in a systematic manner. Based on these results, we show that the PKA-phosphorylated WW is unable to bind a phosphorylated Tau peptide substrate. We next investigate the structural and dynamical perturbations that explain the loss of function due to the phosphorylation. Whereas the triple-stranded conformation of the WW is not changed upon phosphorylation of S16, it does however induce a loss of flexibility of the phospho-binding region as evidenced by changes in NMR relaxation parameters. A model of the phospho-WW domain shows a novel hydrogen bond network as a consequence of the phosphate moiety on S16 that stabilizes the binding-loop.

## Materials and methods

### Production of $^{15}$N/$^{13}$C- or $^{15}$N-labeled WW domain of Pin1 in *Escherichia coli*

The WW domain (residue 5–41 of human Pin1) was produced fused to a N-terminus GST tag in *E. coli* BL21(DE3) strain carrying the WW-pGEX-4T-3 recombinant plasmid. Cells were grown at 37 °C in a M9 minimal medium containing 4 g/L glucose or 2 g/L [$^{13}C_6$]-glucose for expression of $^{13}$C-labeled proteins, 1 g/L $^{15}$N-ammonium chloride, 1 mM $MgSO_4$, MEM vitamin cocktail (Sigma) and ampicilline (100 mg/L). The induction phase was initiated by addition of 0.5 mM Isopropyl-1-thio-*β*-*D*-galactopyranoside and continued at 31 °C for 3 h. Cells were harvested by centrifugation and the pellet was suspended in Phosphate Buffer Saline, 5 % glycerol, 2 mM dithiothreitol, 10 mM EDTA, 1 % Triton X-100 pH 7.2 complemented with a protease inhibitor cocktail (Complete$^{TM}$, Roche). The cell lysate was obtained by incubation of 0.25 mg/ml lysozyme with the cell suspension in extraction buffer complemented with RNase and DNase and followed by a brief sonication step. The soluble extract was isolated by centrifugation. The GST-fusion protein was purified on Glutathione Sepharose (GE Healthcare). Soluble extracts were incubated for 3 h at 4 °C with 25–100 µl resin per milliliter of soluble extracts. Unbound proteins were extensively washed away with a wash buffer (PBS, 5 % glycerol, 1 % Triton X-100, 10 mM EDTA) and proteins were eluted by digestion with Thrombin protease at 0.1 unit/mg fusion protein in one bead-volume of elution buffer (50 mM Tris–Cl pH 8.0, 150 mM NaCl, 2 % glycerol, 0.1 % NP-40, 5 mM EDTA, 5 mM DTT) at 20 °C for 20 h. Elution from the beads was then done twice with one bead-volume of elution buffer. The pooled fractions were concentrated and purified by reverse phase chromatography on a Source 5RPC column (GE Healthcare) equilibrated in 0.05 % TFA aqueous solution (solution A). Separation of proteins was carried out at room temperature at a flow rate of 2 mL/min using a linear acetonitrile gradient over 40 min from 5 to 40 % solution B (80 % acetonitrile in solution A). Homogeneous fractions as checked by 15 % denaturing polyacrylamide gel electrophoresis and MALDI-TOF MS were pooled and lyophilized.

### Phosphorylation of the WW domain of Pin1 by PKA

The WW domain was dissolved at 10 µM in 10 mL of phosphorylation buffer (50 mM Hepes.KOH pH 8.0, 50 mM NaCl, 12.5 mM $MgCl_2$, 1 mM EDTA) with 0.1 µM PKA enzyme. The phosphorylation reaction was performed at 30 °C for 8 h. The mixture was next purified by reverse phase chromatography under the same conditions as for the WW domain. Homogeneous fractions were lyophilized. The protein sample was estimated to be 99 % WW proteins.

### NMR spectroscopy

For NMR experiments, the WW domains were dissolved at 0.3–0.4 mM in a buffer containing 50 mM $d_{11}$-Tris pH 6.8, 100 mM NaCl, 1 mM EDTA, 1 mM DTT and 5 % $D_2O$. As a dissociation constant of 2 mM was measured between Pin1 and phosphate ions (Bayer et al. 2003), we use in this study the deuterated Tris buffer instead of the usual phosphate buffer for this pH range. $^{1}$H spectra were calibrated with 1 mM sodium 3-trimethylsilyl-3,3′,2,2′-d4-propionate (TSP) as a reference. It should be noticed that 4,4-dimethyl-4-silapentane-1-sulfonic acid (DSS) reference is the more widely used. Since the chemical shift difference between TSP and DSS is a constant under given conditions (TSP resonances are pH-dependent), corrections of chemical shifts given in this study using TSP referencing are of −0.015 ppm for protons as compared to DSS (0 ppm) and −0.12 ppm for $^{13}$C nuclei (Wishart et al. 1995). $^{1}$H-$^{15}$N HSQC spectra were recorded at 600 MHz on $^{15}$N- or $^{15}$N/$^{13}$C-labeled proteins with 64 scans per increment, with 2048 and 256 points in the proton and nitrogen dimension, respectively. Three-dimensional HNCACB and HNCO experiments were recorded for both the WW$^{PKA}$ and the unmodified WW domain as a control, with 8 and 4 scans per increment, respectively, and with 2048 and 94 points in the proton and nitrogen dimensions. Proton and nitrogen spectral widths were 13.9 and 30 ppm centered on 4.7 and 120.0 ppm, respectively. In the carbon dimension, spectral widths of 65.4 and 12.0 ppm centered on 39.7 and

172.5 ppm, sampled with 196 and 112 points, were used for the HNCACB and the HNCO experiments, respectively. HNHA experiments were recorded with 8 scans, and 2048, 208, 114 points in the $^{1}$H, $^{15}$N and $^{1}$H dimensions, respectively. Spectral widths were 14.0 and 11.9 ppm centered on 4.7 ppm for the proton, and 24.9 ppm centered on 118.5 ppm for the nitrogen dimension.

The chemical shift perturbations (Δδ) of individual amide resonances were calculated with the Eq. (1) taking into account the relative dispersion of the proton and nitrogen chemical shifts.

$$\Delta\delta(\text{ppm}) = \sqrt{\Delta\delta(^{1}\text{H})^{2} + 0.2\Delta\delta(^{15}\text{N})^{2}} \quad (1)$$

A titration with a phospho-peptide was carried out at 293 K with the WW$^{PKA}$ domain at 0.2 mM and increasing concentrations of substrate at 0, 0.1, 0.2, 0.4, 0.6, 1, 2, and 4 mM on a 300 MHz-spectrometer equipped with a BBI probe.

A pH titration was performed at 293 K on a 600 MHz-spectrometer on a mixture of $^{15}$N-WW$^{PKA}$ and $^{15}$N/$^{13}$C-WW domains at a concentration of 0.1 and 0.12 mM, respectively. The acquisition of $^{1}$H-$^{15}$N HSQC spectra was performed at three different pH values (6.8, 5.86 and 4.86) in a 50 mM $d_{11}$-Tris buffer where pH were adjusted with concentrated HCl. The subspectra corresponding to each differentially labeled species were obtained from a sequence which uses a double INEPT (Insensitive Nuclei Enhanced by Polarization Transfer) transfer with isotopical discrimination between $^{15}$N{$^{12}$CO} and $^{15}$N{$^{13}$CO} (Golovanov et al. 2007) and water suppression using a watergate (WATER suppression by GrAdient Tailored Excitation) sequence (Piotto et al. 1992).

Quantification of phosphorylation level was calculated from peak integration of resonances in two different WW$^{PKA}$ samples at pH 6.8. To monitor the effect of line broadening on the determination of the percentage of phospho-WW, resonances of WW and phospho-WW were integrated in $^{1}$H-$^{15}$N HSQC spectra of a 1: 0.8 mixture of WW:WW$^{PKA}$ at different pH. Given that the WW$^{PKA}$ sample contains both the phospho-WW and WW forms, the determination of the phosphorylation level from $^{1}$H-$^{15}$N HSQC experiments of the WW:WW$^{PKA}$ mixture follows the Eq. (2), where P is the overall phosphorylation level in the WW: WW$^{PKA}$ mixture, p is the phosphorylation level of the WW$^{PKA}$ sample, [WW$^{PKA}$] and [WW] are the concentrations of WW$^{PKA}$ and WW proteins in the mixture, respectively.

$$p = P \times \frac{[WW^{PKA}] + [WW]}{[WW^{PKA}]} \quad (2)$$

P is calculated with the integration of the peaks corresponding to the phosphorylated and the unphosphorylated forms of the WW as in the Eq. (3).

$$P = \frac{A^{phospho-WW}}{A^{phospho-WW} + A^{WW}} \quad (3)$$

$A^{\text{phospho}-\text{WW}}$ and $A^{\text{WW}}$ correspond to the integration of the resonance of a given residue in the phosphorylated and the unphosphorylated form, respectively.

For the 2D NOESY, relaxation and water exchange experiments, WW and WW$^{PKA}$ samples were prepared at 660 and 940 μM, respectively, in 50 mM $d_{11}$-Tris.Cl pH 6.0, 25 mM NaCl, 2.5 mM EDTA, 10 % $D_2O$. For $^{15}$N relaxation and water exchange experiments, data were acquired at 293 K with spectral widths of 14.0 and 52.0 ppm centered on 4.7 and 106.0 ppm in $^{1}$H and $^{15}$N dimensions, respectively, with 2048 points in the detection dimension with 8 scans (for T1 measurements), 16 scans (for T2 and $^{15}$N-NOEs measurements) or 32 scans (for water exchange measurements). Two-dimensional $^{1}$H-$^{1}$H NOESY experiments with 300 ms mixing time, and spectral width of 14.0 and 12.6 ppm in F2 and F1 dimensions, respectively, both centered on 4.7 ppm, were acquired with 2048 points in both dimensions at 293 K with 16 scans and 16 dummy scans. For T1 measurements, mixing times of 10, 100, 200, 400, 600, 800, 1,000, 1,200, 1,500 and 2,000 ms were used. For T2 measurements, mixing times of 16, 32, 63, 95, 126, 158, 189 and 252 ms were used. A proton presaturation delay of 4 s was used for $^{15}$N-heteronuclear NOE experiments. The water exchange rate of backbone amide protons and arginine Hε side chain protons have been measured using the phase-modulated CLEAN chemical Exchange (CLEANEX-PM) experiment (Hwang et al. 1998) with mixing times of 1, 3, 8, 16, 32, 48, 64, 81, 97, 114, 130, 146, 162, 178, 194 ms. The exchange rate constants k were derived from the equation as described (Hwang et al. 1998). Data were fitted to the Eq. (4) were $R_{1water}$ is the longitudinal relaxation rate of water, $R_{1app}$ the apparent longitudinal relaxation rate and k the exchange rate constant. Here, the water R1 was set to 9 $s^{-1}$ ($T_{1water}$ = 111 ms) allowing the calculation of the k values (Figure S1) for each exchangeable amide proton or arginine side chain.

$$\text{intensity}(t) = \text{Cte} \times \left[\exp^{-\text{R1water}\cdot t} - \exp^{-(\text{R1app}+k)\cdot t}\right] \quad (4)$$

## Trypsin digests of WW and PKA-phosphorylated WW domains, and MALDI-TOF MS analyses

Samples of WW domain in its un- and PKA-phosphorylated forms were dissolved at 1 mg/ml in 50 mM ammonium bicarbonate and incubated for 1, 2, 6 or 18 h at 37 °C with 1:100$^{e}$ trypsin (w/w). Samples were then lyophilized, dissolved in water and analyzed with the α-cyano-4-hydroxycinnamic acid matrix. MALDI-TOF MS analyses were performed on a Voyager DE-STR spectrometer

(Applied Biosystems). Detection was carried out in a positive ion mode for the unmodified WW domain and both positive and negative modes for the phosphorylated WW samples.

### Molecular dynamics simulation of the phospho-binding loop of the phospho-WW domain

Simulations were performed using the CAChe software (Fujitsu Limited, Tokyo) with the MM3 force field. Starting from the NMR structure of the apo-WW domain of Pin1 (PDB ID: 1I6C) (Wintjens et al. 2001) and incorporation of the di-anionic phosphoryl group on S16, preliminary energy minimization was accomplished with 1,000 steps of conjugate-gradient algorithm on the protein loop from residues M15–Y23, the rest of the protein being locked. A first molecular dynamics (MD) simulation was then performed *in vacuo* for 50 ps, whereas the final simulated annealing steps (20 ps at high temperature and 50 ps at lower temperature) were carried out using an explicit water model.

## Results

### Identification of the PKA phosphorylation site

The phosphorylated form of the Pin1 WW domain, hereby called the phospho-WW domain, was obtained in vitro by incubation of the WW domain with purified PKA enzyme for 8 h at 30 °C followed by a purification of the crude phosphorylation mixture by reverse phase chromatography. Analysis of the purified $WW^{PKA}$ domain by MALDI-TOF MS indicates the presence of a single phosphorylation site (Fig. 1a), but does not identify the modified residue. MALDI-TOF MS analysis of trypsin digests performed on both the unmodified and PKA-phosphorylated WW domains (Fig. 1b) on the other hand confirm the phosphorylation of S16 (Lu et al. 2002). Signals at m/z values of 393.14 and 549.27 Da corresponding to $MS^{16}R$ and $RMS^{16}R$ peptides around the S16 residue, respectively, are detected in the unmodified WW domain, the former being also detected in the PKA-phosphorylated WW sample. Signals of peptides with a mass increment of +80 Da were detected only in the PKA-phosphorylated WW sample both in positive and negative ion modes and match with the incorporation of a phosphate group. These results unambiguously confirm the presence of a phosphate group on the S16 residue (Fig. 1; Table 1). It should be noted that in case of phosphorylation on S18 or S19 we would not have been able to distinguish one or the other by this method, as trypsin digest could not generate individual peptides in the absence of an arginine residue separating both serine.

The $^{1}H$-$^{15}N$ HSQC spectrum of the $WW^{PKA}$ domain shows two sets of resonances corresponding to the phosphorylated and the unphosphorylated forms of the WW domain. The subspectrum of the unmodified form is significantly weaker confirming that phosphorylation by PKA is almost complete. A mapping of the chemical shift perturbations upon PKA phosphorylation was performed at a pH value of 5.86 (Fig. 2) since severe broadening of the WW resonances at pH values higher than 6.4 leads to a loss of R17 to S19 resonances. Line broadening of these loop resonances and changes related to the phosphorylation state of the WW domain have been further analyzed into details (see below). The chemical shift mapping shows that several residues, grouped in two main regions are affected (Fig. 2).

A first region is the whole phospho-binding loop between β1 and β2 strands, encompassing residues M15 to R21. A second group contains resonances corresponding to residues Y23 and E35, localized in the β2 strand and in the C-terminal loop. In peptides or disordered proteins, phosphorylation induces a large downfield shift of the amide protons of the phosphorylated residues (Theillet et al. 2012), allowing for their easy detection in an otherwise empty region of the $^{1}H$-$^{15}N$ HSQC spectrum. However, in the case of a folded protein such as the WW domain, the corresponding resonances still remain inside the spectral window of amide backbone resonances, and a full assignment of the spectrum is therefore necessary. Based on this assignment, we unexpectedly find that the $^{1}H$-$^{15}N$ largest chemical shift perturbations are detected for S18 and S19 residues and not for S16 (Fig. 2). Shifts of the $^{1}H$-$^{15}N$ cross-peaks compared to the unmodified domain hence cannot unambiguously identify the phosphorylation site of the WW domain.

Comparison with the random coil carbon chemical shift values of either the un- or phosphorylated serine/threonine equally does not lead in a straightforward manner to the identification of the phosphorylation site. As all three serine residues of the loop (S16, S18 and S19) exhibit deviations in $^{13}C\alpha$ values from their random coil values (Fig. 3), it precludes the use of the $^{13}C\alpha$ value as a reliable sensor to probe the phosphorylation site. However, a clear difference in the $^{13}C\beta$ chemical shift of the sole S16 residue between both states points to the latter as the phosphorylation site (Fig. 3). Therefore, in contrast to the situation of IDPs, where the amide proton chemical shift and/or the Cα/Cβ values are unambiguous parameters for identifying the phosphorylated residue, in the case of the folded WW domain, the Cβ value of the phospho-S16 acts as the unique identifying parameter. NMR and MS data thereby confirm the previously identified S16 residue as the unique PKA phosphorylation site within the Pin1 WW domain (Lu et al. 2002).

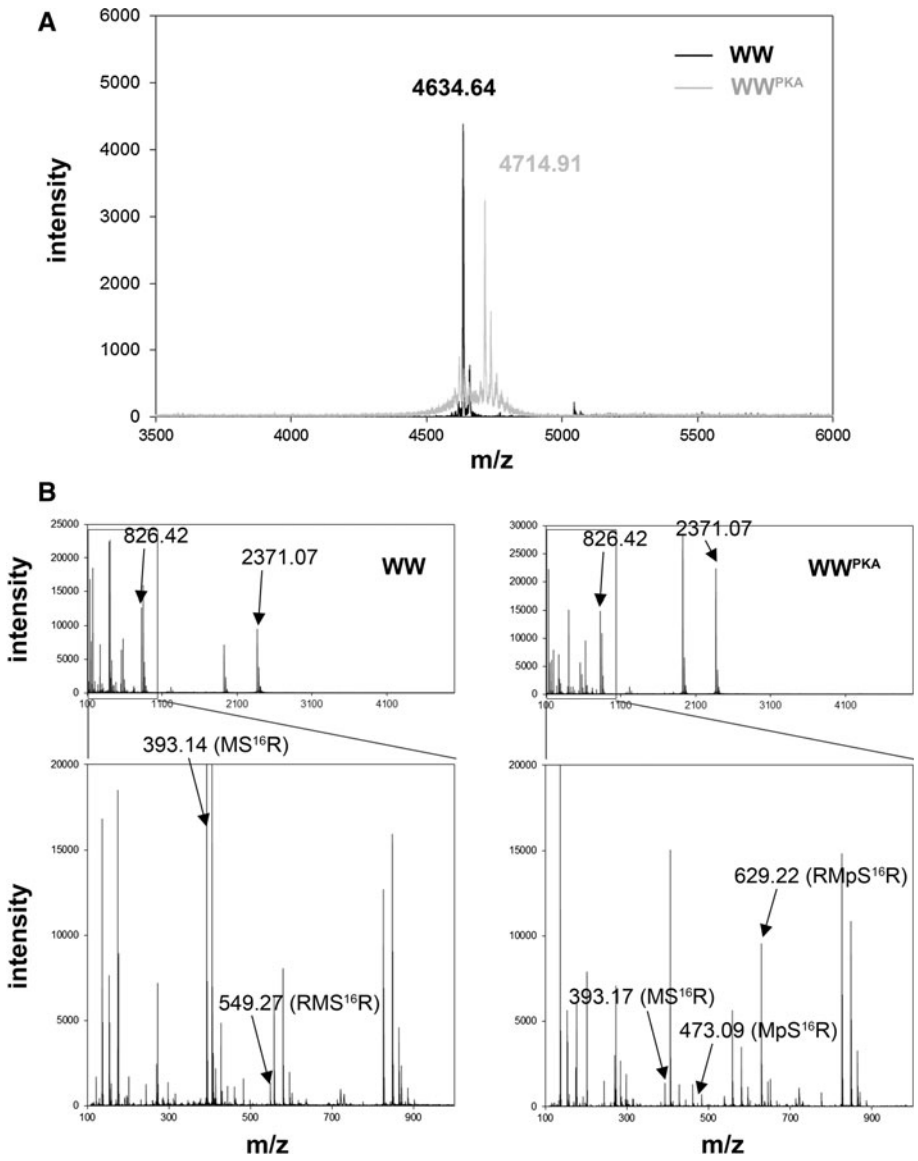


**Fig. 1** Detection and identification of the PKA phosphorylation site on the WW domain by mass spectrometry and trypsin digest. **a** MALDI-TOF mass spectra of the non- (*black*) and PKA-phosphorylated (*grey*) forms of the $^{15}N/^{13}C$-labeled WW domain. **b** MALDI-TOF MS analyses of trypsin digests of the unphosphorylated (WW) and PKA-phosphorylated ($WW^{PKA}$) WW domains in positive ion mode showing the m/z region from 100 to 5000 Da (*upper panels*) and zooms from 100 to 1000 Da (*lower panels*). The molecular ions annotated are $[M + H]^+$ species.*Peaks* are labeled with their monoisotopic masses

**Table 1** Summary of trypsin fragments taking into account no missed cleavage or one missed cleavage in the region of interest

| Non phosphorylated | | Phosphorylated | | Primary sequence | Number of missed cleavage |
|---|---|---|---|---|---|
| Average | Monoisotopic | Average | Monoisotopic | | |
| 290.319 | 290.159 | – | – | GSK | 0 |
| 392.479 | 392.184 | 472.459 | 472.150 | $MS^{16}R$ | 0 |
| 405.411 | 405.197 | 485.391 | 485.163 | $S^{18}S^{19}GR$ | 0 |
| 548.667 | 548.285 | 628.647 | 628.251 | $RMS^{16}R$ | 1 |
| 779.875 | 779.370 | 859.855 | 859.337 | $MS^{16}RS^{18}S^{19}GR$ | 1 |
| 825.963 | 825.438 | – | – | LPPGWEK | 0 |
| 2370.523 | 2369.082 | – | – | VYYFNHITNASQWERPSGNS | 0 |

Average and monoisotopic masses are given. Masses of the corresponding fragments in their phosphorylated form were calculated only for those from the loop containing the three potential phosphorylated serine residues at positions 16, 18 or 19

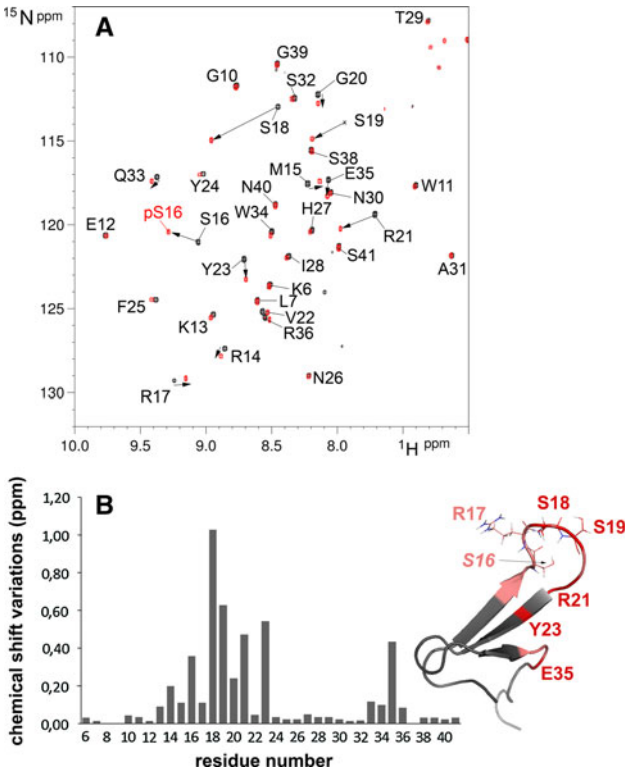


**Fig. 2** Mapping of the PKA phosphorylation site of Pin1 WW domain. **a** $^{1}$H-$^{15}$N HSQC spectra of the WW (*black*) and the PKA-phosphorylated WW (*red*) domain acquired at pH 5.86 allowing the detection of the loop resonances otherwise unobservable at higher pH in the unphosphorylated form. **b** $^{1}$H-$^{15}$N combined chemical shift variations upon PKA phosphorylation of WW domain along the primary sequence, calculated using Eq. (1) and mapped on the WW 3D structure (PDB ID 1I6C). Residues with variations greater than 0.4 ppm are colored in *red* and those comprised between 0.1 and 0.4 ppm in *pink*

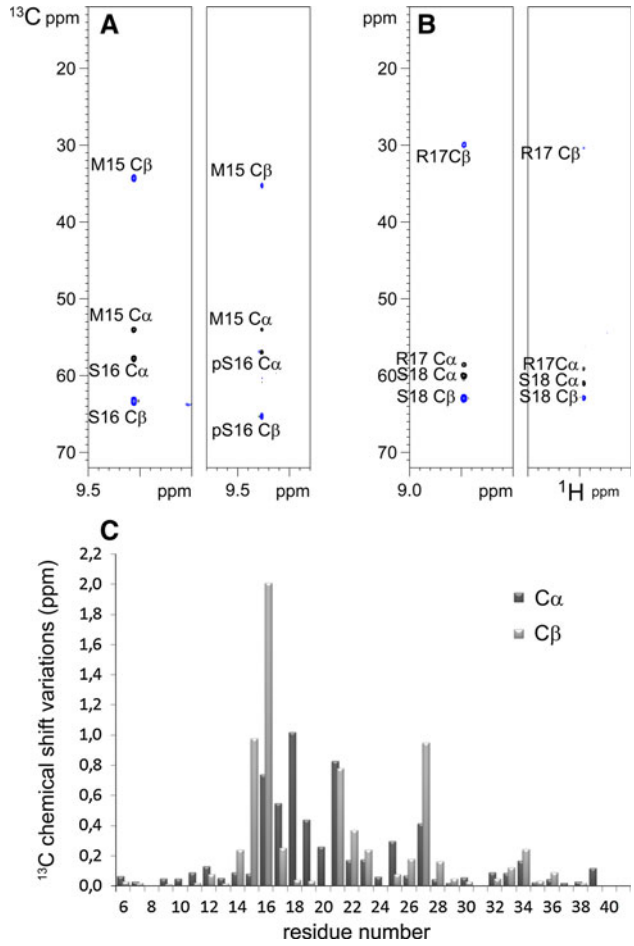


**Fig. 3** Effect of phosphorylation on $^{13}$C chemical shifts. **a** and **b** $^{13}$C strips from HNCACB experiments acquired on $^{15}$N/$^{13}$C-WW (**a** and **b**, *left panels*) and on $^{15}$N/$^{13}$C-WW$^{PKA}$ (**a** and **b**, *right panels*) for Ser16 (**a**) and Ser18 (**b**) residues. **c** Graphical representation of differences of $^{13}$Cα (*dark grey bars*) and $^{13}$Cβ (*light grey bars*) chemical shifts between the non- and the PKA-phosphorylated forms of the WW domain along the primary sequence

## Alternative detection of phosphorylation in WW domain and identification of phosphorylation-related residues by pH titration

The phosphate group carried by serine or threonine residues can experience different ionization states. The transition from the mono- to the dibasic form is pH-dependent and characterized by a pKa value that falls around 6.03 for phospho-serine and 6.34 for phospho-threonine (Bienkiewicz and Lumb 1999). Thus, NMR spectra of phosphorylated peptides undergo pH-dependent shifts attributed to protonation changes of the phospho-S/T side chain. Such pH dependent variations of the amide proton chemical shift have proven valuable indicators of phosphorylation in peptides derived from the Erk activation loop (Prabakaran et al. 2011). We therefore tried the same strategy to characterize the phospho-WW domain. We prepared a mixture of unmodified $^{15}$N/$^{13}$C-labeled and PKA-phosphorylated $^{15}$N-labeled WW domains to ensure identical pH conditions during the pH titration. For each pH value (i.e. pH 6.8, 5.86 and 4.86), a $^{1}$H-$^{15}$N HSQC spectrum with isotopic discrimination between $^{15}$N{$^{12}$CO} and $^{15}$N{$^{13}$CO} was recorded enabling the extraction of sub-spectra corresponding to each differentially labeled species. Effect of pH changes on $^{1}$H-$^{15}$N cross-correlation peaks concerns two regions of the WW domain. First, residues around H27 exhibit pronounced chemical shift modifications with identical behavior in both proteins, in agreement with histidine ionization being pH-sensitive in this range of pH values (Fig. 4, left panels). These His-linked pH perturbations are also visible in both proteins in the region center around residue 13 that is in spatial proximity to H27. When we compared the $^{1}$H-$^{15}$N chemical shifts in the HSQC spectrum of the phospho-WW domain, we observed that resonances in the phospho-binding loop are specifically affected by pH changes between 4.86 and 5.86. We were not able to extend the comparison for pH changes towards pH

values of 6.8 for all residues in this loop due to their broadening in the WW domain (Fig. 4). Together with residues S16–R21 of the loop, both Y23 and E35 were also specifically perturbed upon pH titration (Fig. 4, right panels). The reduced changes between pH 6.8 and 5.86 and the marked shift when going from pH 5.86 to 4.86 indicate that the pKa value of phospho-S16 in the WW domain is comprised in this latter range. However, phospho-S16 itself does not exhibit the largest shift when compared to amide resonances of S18, S19, G20 and R21. These data show that a pH titration experiment leaves a potential ambiguity to detect and identify phosphorylation events in folded proteins, as resonances of other residues can be even more affected by changes of the phosphate protonation state.

## Quantification of the phosphorylation level

In the $WW^{PKA}$ sample, integration of the MALDI-TOF MS signals corresponding to WW and phospho-WW at m/z of 4,634.64 and 4,714.91, respectively, gives 85.3 % of phosphorylated form (see Fig. 1a). The MALDI-TOF MS analysis of trypsin digests that identified the phosphorylation site on the phospho-WW domain did not give a similar level of phosphorylation (Fig. 1b). Phosphorylation potentially has an influence on both the trypsin digestion profile and the ionization properties of peptides, and these factors preclude comparison of the MS signals of modified and unmodified peptides as a basis for quantification of the phosphorylation level of the folded protein.

One of the advantages of NMR spectroscopy is its ability to extract peak intensities or integrals for individual resonances in the 1D or 2D HSQC spectra. This can in principle be used to estimate the stoichiometry of the PTM. Here, we investigate this approach on a folded protein domain by measuring the relative integrals for peaks corresponding to the WW and phospho-WW domain in the HSQC spectra of the PKA-phosphorylated WW domain. Broadening of resonances of the loop region in the WW

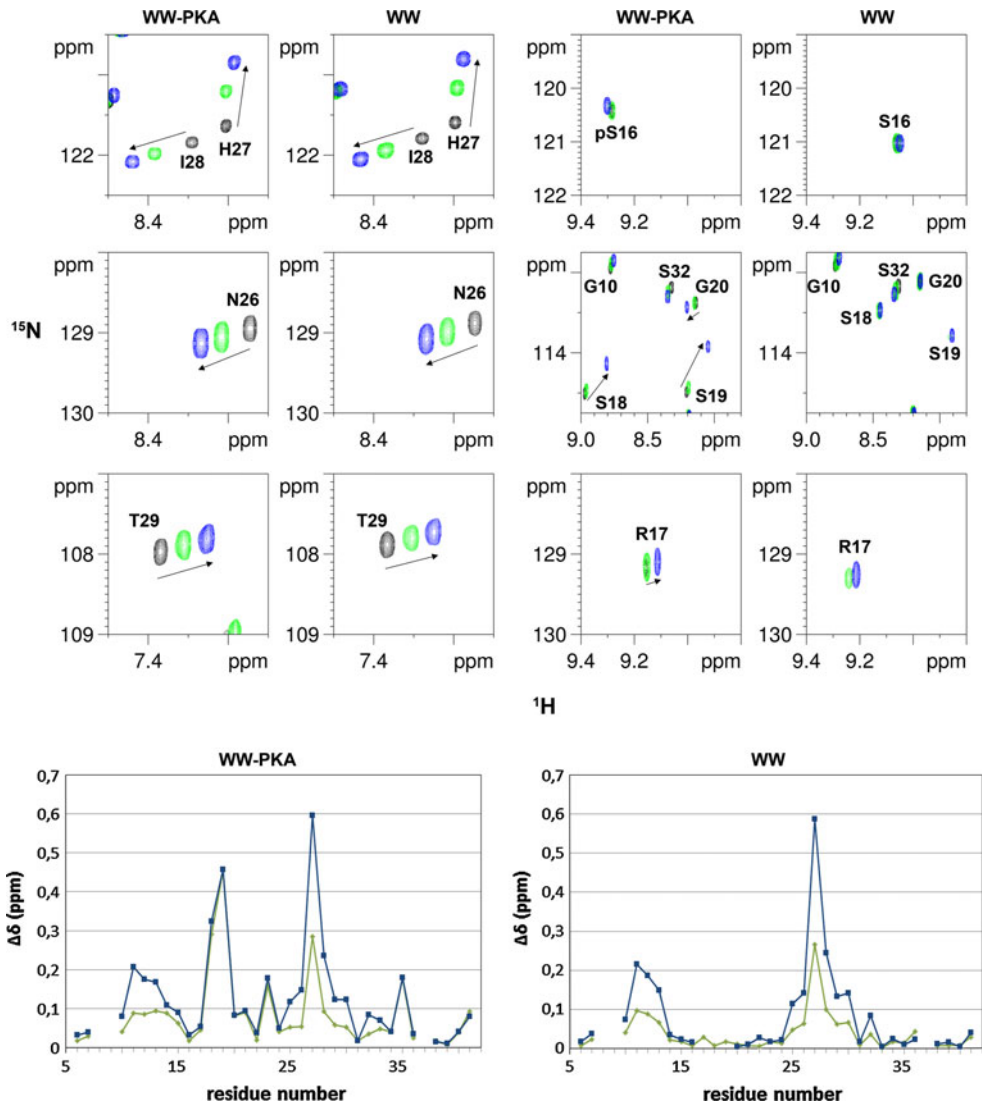


**Fig. 4** pH dependency of the phospho-residue and its neighbours in the phospho-WW domain. (*Upper panels*) Overlay of $^{1}H$-$^{15}N$ HSQC spectra of either the $WW^{PKA}$ or the WW domain at three different pH: 6.8 (*black*), 5.86 (*green*) and 4.86 (*blue*). *Left panels* residues surrounding H27 that have a similar behavior upon pH variations for both proteins. *Right panels* residues surrounding S16 that exhibit a distinct behavior upon pH variations in phospho-WW and WW proteins. (*Lower panels*) Graphical representation of chemical shift displacements for phospho-WW (*left*) and WW (*right*) domains upon pH variation from 4.86 to 5.68 (*green curves*) and from 4.86 to 6.8 (*blue curves*). Residues without data points correspond either to proline residues (position 8, 9 and 37) or residues of the loop (from R17 to S19) that are too broad to be detected at pH 6.8

domain posed an obvious challenge for the quantification, as one could indeed conclude on the basis of these peaks that the sample only contains phospho-WW (Fig. 5). The line broadening is moreover pH-dependent, because lowering the pH restores some intensity for peaks corresponding to the loop residues in the unmodified WW domain. When we take peaks that are distinguishable between both forms but that are further away from the loop, we arrive at an overall phosphorylation level of 90 ± 3 % phosphorylation in the $WW^{PKA}$ domain, in agreement with the MS data on the intact domain. In the $^{1}H$-$^{15}N$ HSQC of binary mixture (1:0.8 WW:$WW^{PKA}$) used to monitor the pH titration, and using the spectrum at the lowest pH, we estimated in a similar manner a phosphorylation level of 35 ± 5 % (Fig. 5b) that indicates a phosphorylation level of 80 ± 10 % for the initial $WW^{PKA}$ sample.

## Effect of WW phosphorylation on its binding activity

The WW domain of Pin1 binds phosphorylated peptide substrates, with a marked specificity for phospho-S/T–P motifs generated by proline-directed kinases. In a previous work, we have evaluated the dissociation constants of several peptides from the neuronal Tau protein for either the full-length Pin1 or the isolated WW domain, and found no selectivity of Pin1 binding for a particular Tau phospho-epitope (Smet et al. 2004). Here, we measure by NMR spectroscopy the binding constant of phospho-WW for a phospho-peptide of the human Tau protein (residues 208–221) phosphorylated on residue T212. We performed a titration of $^{15}N$-labeled $WW^{PKA}$ domain at a constant concentration of 200 μM with increasing amounts of the phospho-peptide. The dissociation constant of the complex was beyond the values accessible by NMR measurements which would need concentrations largely above the limit of solubility of the peptide to reach saturation. In contrast, a binding constant of 100 μM had been measured for the WW domain under the same conditions (Smet et al. 2004) (Fig. 6). Phosphorylation of the WW hence leads to a loss of function on phospho-substrate binding, thereby rationalizing the loss of Pin1 function upon PKA phosphorylation (Lu et al. 2002).

## Dynamical and structural changes of the phospho-binding loop upon phosphorylation

To explore the relationship between WW phosphorylation and its loss of binding capacity, we first considered the structural consequences of phosphate incorporation at position S16. Based on the comparison of Cα and Cβ secondary chemical shifts and $^{3}J$ $H_N$–Hα couplings between the unphosphorylated and the PKA-phosphorylated forms of the WW domain (Fig. 6), we conclude that the triple β-sheet structure is maintained upon PKA phosphorylation. Comparison of the NOE patterns of phospho-WW and WW additionally indicates that no major structural change is induced by phosphorylation (Fig. 7a). Without obvious structural modifications of the WW backbone upon phosphorylation, we compared the relaxation parameters at pH 6.0 (Fig. 8) where all resonances in both WW and phospho-WW domains $^{1}H$-$^{15}N$ HSQC can be detected. As we estimated the pKa of phospho-S16 between pH 4.86 and 5.86, the phospho-S16 is present in its physiological di-anionic state at pH 6.0.

$^{15}N$-R1 and $^{1}H$-$^{15}N$ heteronuclear NOE values of the backbone amide resonances allow distinguishing the strands from the loop regions, but are not significantly different upon phosphorylation. Whereas this is in agreement with the conservation of the overall fold upon phosphorylation, the slight decrease of the overall $^{15}N$-R1 values points towards a higher compactness of the phospho-WW (Fig. 8). However, the selective line broadening of the loop resonances in the unmodified domain is reflected in the selective decrease in $^{15}N$-$R_2$ values of those same loop residues in the phosphorylated WW domain at pH 6.0 (Fig. 8). Because the overall tumbling is not expected to change in view of the overall structure conservation, phosphorylation of S16 hence seems to result in a lessening of exchange broadening on the microsecond-millisecond timescale. This effect is not limited to next neighbours in the WW binding loop but equally expands throughout the β1 strand (Fig. 8).

Comparative measurements of water exchange rates of backbone amide and side chain protons using the phase-modulated CLEAN chemical EXchange experiment show a significant decrease of water exchange upon phosphorylation for most backbone amides from the phospho-binding loop (R17 to S19) but also for the side chain protons of the arginine residues (Fig. 8 and see Supplementary Materials, Figure S1). These reduced water exchange rates could be solely due to the introduction of negative charges in the binding loop of the phosphorylated domain. However, part of the observed changes in water exchange rates could also reflect reduced solvent accessibility accompanying the conformational stabilization. Rearrangement of the hydrogen network previously described for the WW domain when bound to its substrate (Peng et al. 2007) is a third factor in agreement with the reduced water exchange we observe. Both the decrease of microsecond-millisecond movements and the slower water exchange for backbone amides of residues in the binding-loop, and more specifically for residues S16, R17, S18 and S19, account for the decreased line-width of the corresponding resonances in the $^{1}H$-$^{15}N$ HSQC of the phosphorylated domain.

A model of the phospho-WW domain (Fig. 7) shows compaction of the binding-loop region, as a consequence of

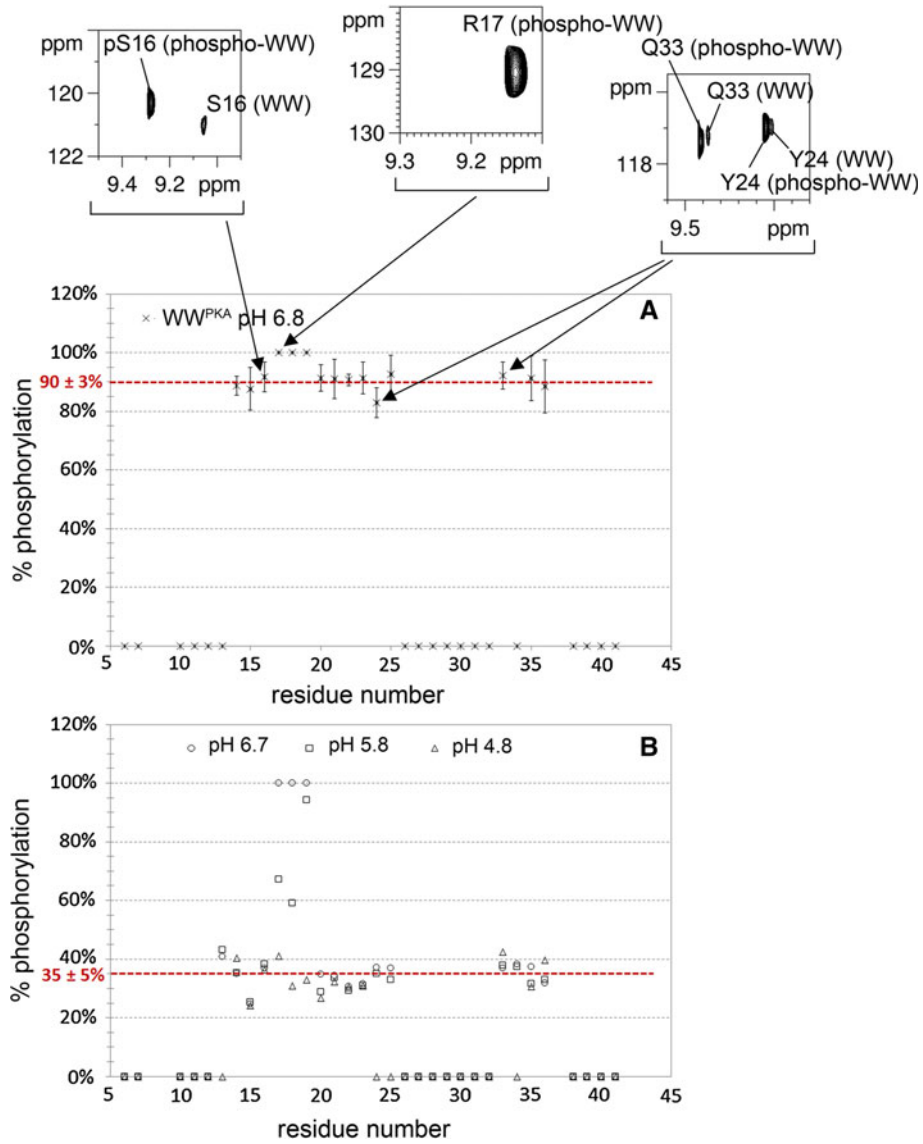


**Fig. 5** Quantification of PKA phosphorylation level in WW domain by NMR. Determination of the phosphorylation level based on integrations of signals corresponding to WW and phospho-WW in the $WW^{PKA}$ sample at pH 6.8 in $^{1}H$-$^{15}N$ HSQC experiments (**a**) or in $^{1}H$-$^{15}N$ HSQC experiments of a WW: $WW^{PKA}$ mixture (ratio 1: 0.8) acquired at different pH (**b**). **a** Resonances of S16, R17, Y24 and Q33 residues from the $^{1}H$-$^{15}N$ HSQC spectrum of the $WW^{PKA}$ sample corresponding either to the phosphorylated (phospho-WW) or unphosphorylated (WW) forms are shown. Calculation of phosphorylation level was done for two different phosphorylation reactions with PKA and mean values are indicated for each residue. Zero values are arbitrarily assigned to residues that have the same chemical shift in both the unphosphorylated and PKA-phosphorylated forms. For residues of the phospho-binding loop (R17–S19), despite different chemical shifts in both forms, the absence of detectable signals at pH 6.8 in the unphosphorylated form lead to an apparent phosphorylation level of 100 % based on these residues. **b** Data acquired at pH 6.7, 5.86 and 4.86 are depicted by *open circles*, *squares* and *triangles*, respectively. The mean phosphorylation level and root mean square deviation were calculated with data excluding values corresponding either to residues that give the same resonances in both WW and $WW^{PKA}$ or residues of the β-hairpin loop that experience severe line broadening (R17–S19). The mean phosphorylation level of 35 ± 5 % was calculated at pH 6.7 and similar values were found at pH 5.86 or 4.86

novel H-bonds between the phosphate moiety and the side chains of R17, R21 and Y23. These could account for the conformational stabilization as witnessed by reduced $^{15}N$-R2 rates and for the reduction of water exchange rates for residues in the binding loop. Moreover, conformational rearrangements of the phospho-binding loop and R21 side chain in this model are in good agreement with the significant chemical shift perturbations observed for the S18, S19, R21 and Y23 $^{1}H$,$^{15}N$ resonances upon PKA phosphorylation (Fig. 2). The novel H-bond of the side chain of R21 to the phospho-S16 in our model will turn it away from the side chain of E35, and hence could additionally

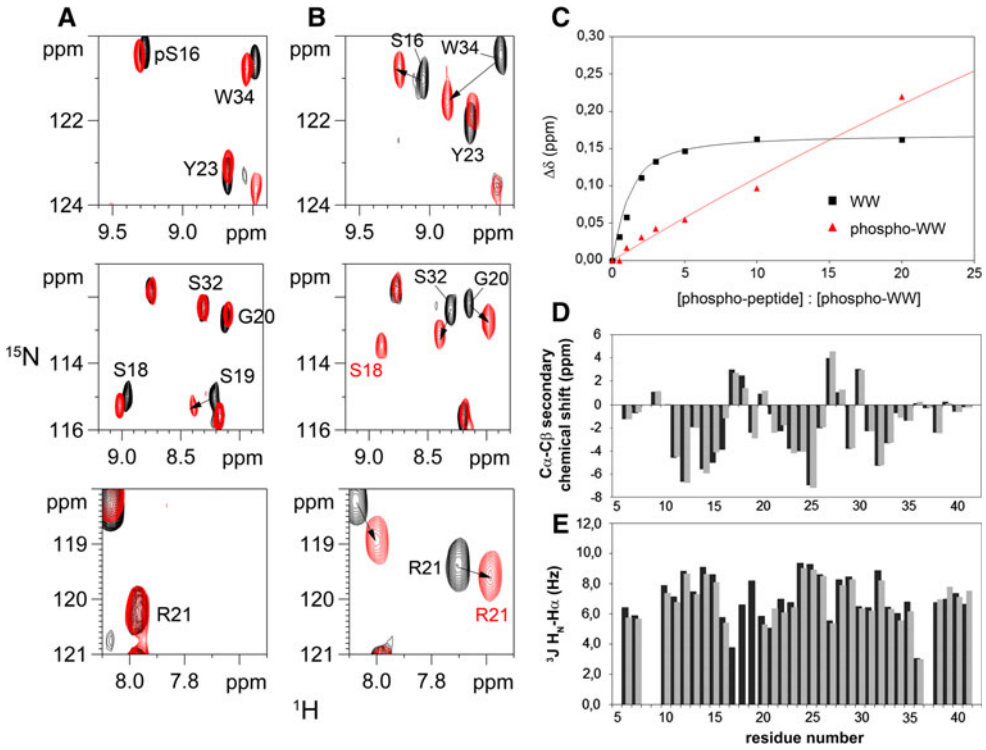


**Fig. 6** Binding activity of the phospho-WW domain of Pin1 to phospho-substrates. (**a**, **b**) Titration of the $^{15}$N-labeled WW$^{PKA}$ (**a**) and WW (**b**) domains with a peptide from human Tau protein (residues 208–221) containing the phospho-Thr212-Pro motif (Smet et al. 2004). $^{1}$H-$^{15}$N HSQC spectra depicted in *black* represent the apo proteins, WW$^{PKA}$ (**a**) or WW (**b**), spectra in *red* represent the proteins in the presence of a 20-fold excess of phospho-peptide. **c** Titration curves for the non- (*black*) and PKA-phosphorylated (*red*) WW domain allowing for the calculation of dissociation constants. **d** Cα – Cβ secondary chemical shifts of the phospho-WW and unmodified WW domains. $^{13}$C chemical shifts values used as references are described in (Wishart and Sykes 1994). **e** $^{3}$J scalar couplings between backbone amide and alpha protons calculated from HNHA experiments. Data of phospho-WW domain are represented in *black bars* and those of unmodified WW domain in *grey bars*

explain the chemical shift perturbation observed for the E35 $^{1}$H,$^{15}$N upon phosphorylation of S16. As the pH value will determine the value of the net charge of the phospho-S16 residue, we furthermore observe for all these residues networked to the phospho-serine that the amide $^{1}$H and $^{15}$N chemical shifts titrate with pH (Fig. 4). The conformation of the R17, S18, S19 and Y23 residues in the phospho-WW is similar to the one they adopt in the loop of the WW domain bound to a phospho-peptide substrate (Fig. 7d and see Supplementary Materials, Figure S2). In support of this, chemical shift variations for residues R17 to S19 are similar in direction when we compare the phospho-WW domain and the WW domain complexed to a phospho-peptide (see Figs. 2a and 6b for comparison). They are however distinct for Y23 and R21, which can be rationalized by the role that Y23 plays in accommodating the proline moiety of the phospho-S–P ligand (Verdecia et al. 2000; Wintjens et al. 2001) while its side chain directly points to the S16 phosphate moiety in our model structure. Equally, the R21 side chain conformation in the structure of the complex points away from the phosphorylated serine side chain of the peptide ligand (Verdecia et al. 2000; Wintjens et al. 2001) whereas in our model, it is involved in the positioning of the phospho-S16 side chain.

## Discussion

To better understand the mechanism of regulation of Pin1 function through phosphorylation of its WW domain, and increase our general understanding of functional regulation by phosphorylation, we present here a detailed structural and functional study of its phosphorylated WW domain. At first, we evaluated the use of NMR to detect, identify and quantify the phosphorylation event after in vitro phosphorylation by the PKA kinase. Although phosphorylation of globular proteins is mostly directed to disordered regions or flexible loops, the fact that those are embedded in the three-dimensional structure renders the characterization of phosphorylation less straightforward than in case of IDPs (Landrieu et al. 2006; 2010; Lippens et al. 2008; Theillet et al. 2012). Indeed, we found that no significant shift of $^{1}$H, $^{13}$C and $^{15}$N goes significantly beyond the usual range observed in folded proteins, and hence can

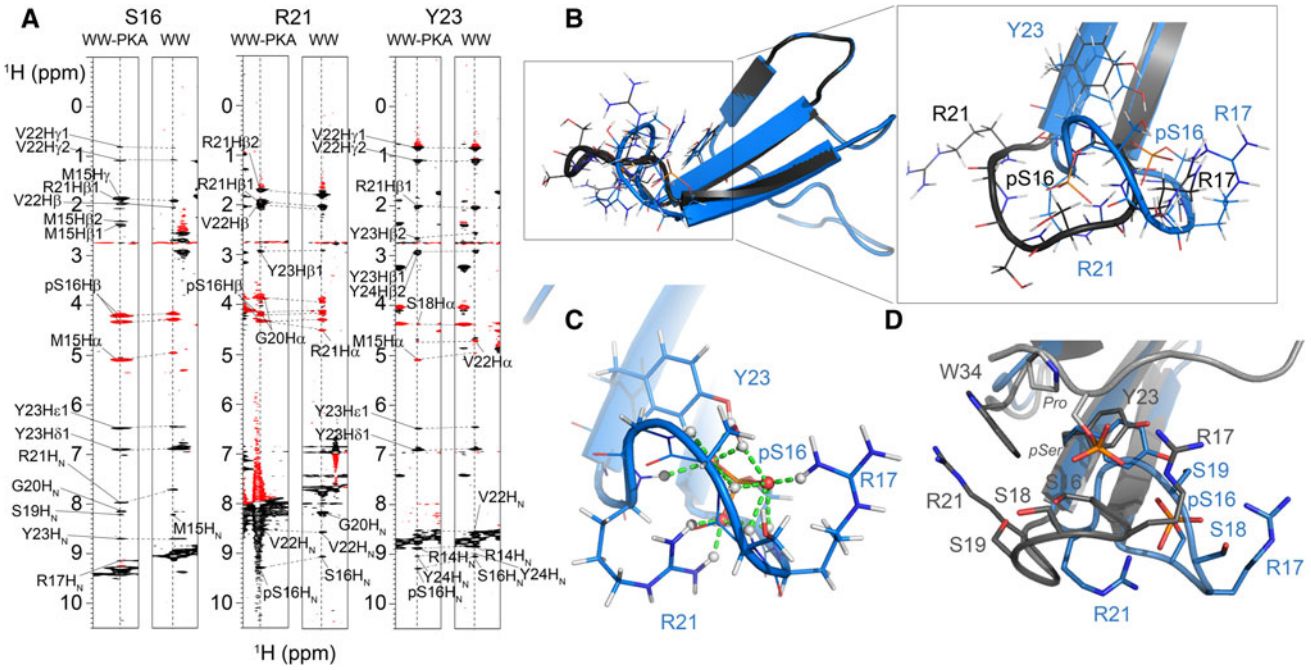


**Fig. 7** Structural model of the phospho-WW domain. **a** Comparison of $^{1}$H strips from the $^{1}$H-$^{1}$H $^{15}$N-filtered NOESY experiments for the residues S16, R21 and Y23 of the WW (*right panels*) and the WW-PKA domains (*left panels*). **b** Comparison of the structure of the WW (*grey*, PDB ID : 1I6C) (Wintjens et al. 2001) and the model structure of the phospho-WW based on the structure of the unphosphorylated form and molecular dynamics simulations restrained to M15 to Y23 residues (*blue*) highlighting a compaction of the phospho-binding loop upon PKA phosphorylation. **c** Close-up of the phospho-binding loop of the phospho-WW domain showing the intramolecular contacts with the phosphate moiety. Both R17 and R21 side chains guanidium moieties establish intramolecular contacts with the phospho-S16 together with the phenol group of the Y23 that probably participate to the compactness of the phosphorylated WW domain. This conformation explains the decrease of water exchange rates for the residues of the loop in the phospho-WW as compared to the WW domain as well as the overall R1 decrease and the reduced R2 values of the residues of the loop. **d** Comparison of the modeled structure of phospho-WW (*blue*) with the structure of the WW domain bound to a phospho-peptide (*grey*, PDB ID: 1F8A) (Verdecia et al. 2000). In this latter structure, residues of the WW domain are indicated in regular *grey* characters and those of the phospho–S–P motif of the peptide substrate in *italic*

unambiguously identify a specific serine residue as the phosphorylation site. The $^{1}$H-$^{15}$N chemical shift mapping when comparing both the unmodified and PKA-phosphorylated WW resonances only highlighted the phospho-binding loop as the region containing the phosphorylation site. However, all the three serine residues present in this loop show pronounced backbone amide chemical shift changes upon PKA phosphorylation, with S18 residue exhibiting the largest chemical shift variations. This clearly argues against the identification of the phospho-site on the basis of the sole $^{1}$H-$^{15}$N chemical shift mapping (Fig. 2). The site identification came from the precise comparison of $^{13}$C values between the unmodified and phosphorylated WW domains, whereby the Cβ of S16 appears to be solely affected by phosphorylation (Fig. 3). Whereas this result is in agreement with MS, we should notice that this latter approach would not necessarily be able to discriminate between S18 and S19 residues as putative phosphorylation sites, given their adjacent positions. While peptide-based MS is conditioned by the presence of a protease cleavage site between the putative phosphorylation positions, NMR identification based on the characteristic shift of the phospho-serine $^{13}$Cβ carbon should function independently of the primary sequence, in a non-destructive manner.

Since $^{1}H_N$ and $^{15}$N chemical shifts are not valuable *indicators* of phosphorylation events in folded proteins, we investigated whether the pH dependency of protein resonances in the range of pH around the pKa value of phospho-S/T residues could play this role. In the absence of stable tertiary structure, the intramolecular hydrogen bond between the phospho-serine phosphate moiety and its own amide hydrogen is the underlying factor that determines the pH dependence of the amide proton chemical shift (Du et al. 2005). In the case of the WW loop, we observe the most pronounced pH dependence for the amide proton of S18, suggesting that the tertiary structure imposes an inter- rather than intra-residue hydrogen bond (see the modeled structure, Fig. 7c). As a result, the pH titration behaviour of the backbone amide resonance is a second invalid parameter to identify the site of phosphate incorporation. Finally, NMR as a tool to measure the stoichiometry of the PTM equally requires some caution in the case of a folded

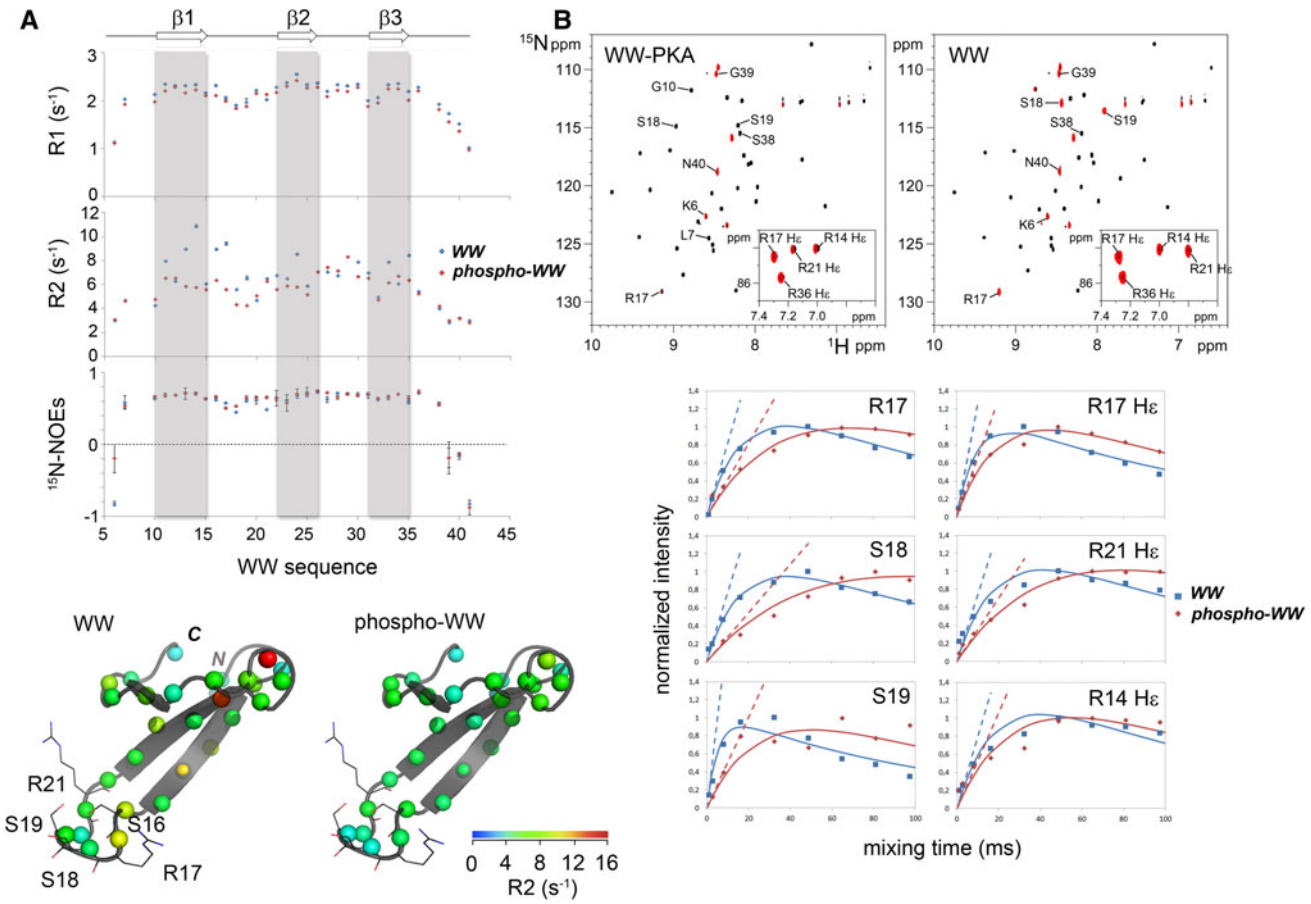


**Fig. 8** Dynamics of the phospho-WW domain. **a** Comparison of dynamics parameters of the WW and the phospho-WW domains. *Upper panel*, representation of R1, R2 and $^{15}$N-NOEs values along the Pin1 WW primary sequence for WW (*blue*) and WW-PKA (*red*) domains. Dynamics parameters were measured at pH 6.0 allowing the detection of the resonances of the phospho-binding loop (residue 16–21) in both samples. *Arrows* above the graphics indicate the position of each β-strand. Note that the R2 values for N26 and T29 residues in the WW domain are not shown and are of 14.5 and 16.5 $s^{-1}$, respectively. *Lower panel*, the R2 values color coded on the WW structure (PDB ID 1F8A) where each sphere is a backbone amide nitrogen. **b** Water exchange measurements using the CLEAN chemical EXchange (CLEANEX) experiments. *Upper panel*, comparison of the $^{1}$H-$^{15}$N HSQC of the WW and WW-PKA domains (*black*) with the CLEANEX experiments with a mixing time of 50 ms (*red*). *Lower panel*, normalized intensity variations of the signals of WW (*blue*) versus phospho-WW (*red*) for different mixing times for the loop NH signals (R17, S18, S19) and the Hε arginine side chains (R17, R21 and R14). Fitted CLEANEX exchange curves (*plain lines*) were calculated as described (Hwang et al. 1998). Initial velocities (*dotted lines*) were calculated from fitted curves allowing the determination of the water exchange rate parameter k (see Supplementary Materials, Figure S1)

domain, especially when it induces modifications such as the loop stabilization and decrease in water exchange rate of backbone amides that we observe for the phospho-WW domain. However, when we compare peak integrals in $^{1}$H-$^{15}$N HSQC for the residues outside of this loop region in the $WW^{PKA}$ sample, we found good agreement with the MALDI-TOF MS on the intact proteins, and deduced a phosphorylation yield of 90 ± 3 %.

In addition to its analytical capacities, NMR spectroscopy is powerful to characterize the structural, dynamical and functional consequences of phosphorylation. PKA phosphorylation of the WW leads to a loss of its binding capacity to a phosphorylated Tau peptide, despite the overall triple β-sheet structure of the WW module being conserved (Fig. 6). This suggests modulation of the WW binding activity at another level. Protein motions such as loop flexibility are known to be involved in the control of enzymatic functions, ligand binding or protein–protein interactions (Baldwin and Kay 2009; Eisenmesser et al. 2005; Kay 2005; Mittermaier and Kay 2006). Conformational exchange and flexibility of the binding-loop region of the WW domain were indeed shown to be an important parameter for the binding affinity and specificity of the WW domain for phosphorylated substrates (Peng et al. 2007; Sharpe et al. 2007). The observed restriction in the backbone dynamics of this region once the WW domain is phosphorylated on S16, most pronounced on the μs-ms timescale, is thus a first factor that might participate in the

observed decrease of affinity for binding. Introduction of a phosphate moiety on S16 further limits the availability of R17, the essential residue for the phosphate binding of the protein partner. Our data hence suggest that the conformational and dynamical changes of the phospho-binding loop upon S16 phosphorylation resemble the structural adaptation occurring when a phosphorylated peptide substrate binds to the WW domain (see Fig. 7d and Supplementary Materials, Figure S2). Such conformational mimicking could explain the loss of function of the Pin1 WW domain in its PKA-phosphorylated state. Both mechanisms of gain of conformational rigidity and compactness together with the phosphate moiety itself occupying the position of the incoming phospho-S/T will lead to a phospho-WW domain unable to bind other phosphoproteins.

**Acknowledgments** We thank Professor H. Schwalbe (Frankfurt, Germany) for a kind gift of the purified PKA enzyme. The NMR facilities are funded by the the European community, the Centre National de la Recherche Scientifique (CNRS), the Région Nord-Pas de Calais (France), the University of Lille 1 and the Institut Pasteur de Lille. The Mass Spectrometry facilities are funded by the European community (FEDER), the Région Nord-Pas de Calais (France), the IBISA network, the CNRS, and the University of Lille 1.

## References

Ando K, Dourlen P, Sambo AV, Bretteville A, Belarbi K, Vingtdeux V, Eddarkaoui S, Drobecq H, Ghestem A, Begard S, Demey-Thomas E, Melnyk P, Smet C, Lippens G, Maurage CA, Caillet-Boudin ML, Verdier Y, Vinh J, Landrieu I, Galas MC, Blum D, Hamdane M, Sergeant N, Buee L (2012) Tau pathology modulates Pin1 post-translational modifications and may be relevant as biomarker. Neurobiol Aging 34(3):757–769

Andrew CD, Warwicker J, Jones GR, Doig AJ (2002) Effect of phosphorylation on alpha-helix stability as a function of position. Biochemistry 41(6):1897–1905

Arosio B, Bulbarelli A, Bastias Candia S, Lonati E, Mastronardi L, Romualdi P, Candeletti S, Gussago C, Galimberti D, Scarpini E, Dell'Osso B, Altamura C, MacCarrone M, Bergamaschini L, D'Addario C, Mari D (2012) Pin1 contribution to Alzheimer's disease: transcriptional and epigenetic mechanisms in patients with late-onset Alzheimer's disease. Neuro Degener Dis 10(1–4): 207–211

Bai Y, Milne JS, Mayne L, Englander SW (1993) Primary structure effects on peptide group hydrogen exchange. Proteins 17(1): 75–86

Baker JM, Hudson RP, Kanelis V, Choy WY, Thibodeau PH, Thomas PJ, Forman-Kay JD (2007) CFTR regulatory region interacts with NBD1 predominantly via multiple transient helices. Nat Struct Mol Biol 14(8):738–745

Balastik M, Lim J, Pastorino L, Lu KP (2007) Pin1 in Alzheimer's disease: multiple substrates, one regulatory mechanism? Biochim Biophys Acta 1772(4):422–429

Baldwin AJ, Kay LE (2009) NMR spectroscopy brings invisible protein states into focus. Nat Chem Biol 5(11):808–814

Bayer E, Goettsch S, Mueller JW, Griewel B, Guiberman E, Mayr LM, Bayer P (2003) Structural analysis of the mitotic regulator hPin1 in solution: insights into domain architecture and substrate binding. J Biol Chem 278(28):26183–26193

Bienkiewicz EA, Lumb KJ (1999) Random-coil chemical shifts of phosphorylated amino acids. J Biomol NMR 15(3):203–206

Bulbarelli A, Lonati E, Cazzaniga E, Gregori M, Masserini M (2009) Pin1 affects Tau phosphorylation in response to Abeta oligomers. Mol Cell Neurosci 42(1):75–80

Du JT, Li YM, Wei W, Wu GS, Zhao YF, Kanazawa K, Nemoto T, Nakanishi H (2005) Low-barrier hydrogen bond between phosphate and the amide group in phosphopeptide. J Am Chem Soc 127(47):16350–16351

Eisenmesser EZ, Millet O, Labeikovsky W, Korzhnev DM, Wolf-Watz M, Bosco DA, Skalicky JJ, Kay LE, Kern D (2005) Intrinsic dynamics of an enzyme underlies catalysis. Nature 438(7064): 117–121

Eto M, Kitazawa T, Matsuzawa F, Aikawa S, Kirkbride JA, Isozumi N, Nishimura Y, Brautigan DL, Ohki SY (2007) Phosphorylation-induced conformational switching of CPI-17 produces a potent myosin phosphatase inhibitor. Structure 15(12): 1591–1602

Golovanov AP, Blankley RT, Avis JM, Bermel W (2007) Isotopically discriminated NMR spectroscopy: a tool for investigating complex protein interactions in vitro. J Am Chem Soc 129(20): 6528–6535

Hamdane M, Smet C, Sambo AV, Leroy A, Wieruszeski JM, Delobel P, Maurage CA, Ghestem A, Wintjens R, Begard S, Sergeant N, Delacourte A, Horvath D, Landrieu I, Lippens G, Buee L (2002) Pin1: a therapeutic target in Alzheimer neurodegeneration. J Mol Neurosci 19(3):275–287

Hwang TL, van Zijl PC, Mori S (1998) Accurate quantitation of water-amide proton exchange rates using the phase-modulated CLEAN chemical EXchange (CLEANEX-PM) approach with a Fast-HSQC (FHSQC) detection scheme. J Biomol NMR 11(2): 221–226

Iakoucheva LM, Radivojac P, Brown CJ, O'Connor TR, Sikes JG, Obradovic Z, Dunker AK (2004) The importance of intrinsic disorder for protein phosphorylation. Nucleic Acids Res 32(3): 1037–1049

Johnson LN, Barford D (1993) The effects of phosphorylation on the structure and function of proteins. Annu Rev Biophys Biomol Struct 22:199–232

Kay LE (2005) NMR studies of protein structure and dynamics. J Magn Reson 173(2):193–207

Landrieu I, Lacosse L, Leroy A, Wieruszeski JM, Trivelli X, Sillen A, Sibille N, Schwalbe H, Saxena K, Langer T, Lippens G (2006) NMR analysis of a Tau phosphorylation pattern. J Am Chem Soc 128(11):3575–3583

Landrieu I, Leroy A, Smet-Nocca C, Huvent I, Amniai L, Hamdane M, Sibille N, Buee L, Wieruszeski JM, Lippens G (2010) NMR spectroscopy of the neuronal tau protein: normal function and implication in Alzheimer's disease. Biochem Soc Trans 38(4): 1006–1011

Liou YC, Sun A, Ryo A, Zhou XZ, Yu ZX, Huang HK, Uchida T, Bronson R, Bing G, Li X, Hunter T, Lu KP (2003) Role of the prolyl isomerase Pin1 in protecting against age-dependent neurodegeneration. Nature 424(6948):556–561

Lippens G, Landrieu I, Hanoulle X (2008) Studying posttranslational modifications by in-cell NMR. Chem Biol 15(4):311–312

Lonati E, Masserini M, Bulbarelli A (2011) Pin1: a new outlook in Alzheimer's disease. Curr Alzheimer Res 8(6):615–622

Lu KP, Hanes SD, Hunter T (1996) A human peptidyl-prolyl isomerase essential for regulation of mitosis. Nature 380 (6574): 544–547

Lu PJ, Wulf G, Zhou XZ, Davies P, Lu KP (1999) The prolyl isomerase Pin1 restores the function of Alzheimer-associated phosphorylated tau protein. Nature 399(6738):784–788

Lu PJ, Zhou XZ, Liou YC, Noel JP, Lu KP (2002) Critical role of WW domain phosphorylation in regulating phosphoserine binding activity and Pin1 function. J Biol Chem 277(4):2381–2384

Ma SL, Pastorino L, Zhou XZ, Lu KP (2012) Prolyl isomerase Pin1 promotes amyloid precursor protein (APP) turnover by inhibiting glycogen synthase kinase-3beta (GSK3beta) activity: novel mechanism for Pin1 to protect against Alzheimer disease. J Biol Chem 287(10):6969–6973

Mittermaier A, Kay LE (2006) New tools provide new insights in NMR studies of protein dynamics. Science 312(5771):224–228

Ohki S, Eto M, Kariya E, Hayano T, Hayashi Y, Yazawa M, Brautigan D, Kainosho M (2001) Solution NMR structure of the myosin phosphatase inhibitor protein CPI-17 shows phosphorylation-induced conformational changes responsible for activation. J Mol Biol 314(4):839–849

Pastorino L, Sun A, Lu PJ, Zhou XZ, Balastik M, Finn G, Wulf G, Lim J, Li SH, Li X, Xia W, Nicholson LK, Lu KP (2006) The prolyl isomerase Pin1 regulates amyloid precursor protein processing and amyloid-beta production. Nature 440(7083):528–534

Peng T, Zintsmaster JS, Namanja AT, Peng JW (2007) Sequence-specific dynamics modulate recognition specificity in WW domains. Nat Struct Mol Biol 14(4):325–331

Piotto M, Saudek V, Sklenar V (1992) Gradient-tailored excitation for single-quantum NMR spectroscopy of aqueous solutions. J Biomol NMR 2(6):661–665

Prabakaran S, Everley RA, Landrieu I, Wieruszeski JM, Lippens G, Steen H, Gunawardena J (2011) Comparative analysis of Erk phosphorylation suggests a mixed strategy for measuring phospho-form distributions. Mol Syst Biol 7:482

Pufall MA, Lee GM, Nelson ML, Kang HS, Velyvis A, Kay LE, McIntosh LP, Graves BJ (2005) Variable control of Ets-1 DNA binding by multiple phosphates in an unstructured region. Science 309(5731):142–145

Pullen K, Rajagopal P, Branchini BR, Huffine ME, Reizer J, Saier MH Jr, Scholtz JM, Klevit RE (1995) Phosphorylation of serine-46 in HPr, a key regulatory protein in bacteria, results in stabilization of its solution structure. Protein Sci 4(12):2478–2486

Ranganathan R, Lu KP, Hunter T, Noel JP (1997) Structural and functional analysis of the mitotic rotamase Pin1 suggests substrate recognition is phosphorylation dependent. Cell 89(6):875–886

Rangasamy V, Mishra R, Sondarva G, Das S, Lee TH, Bakowska JC, Tzivion G, Malter JS, Rana B, Lu KP, Kanthasamy A, Rana A (2012) Mixed-lineage kinase 3 phosphorylates prolyl-isomerase Pin1 to regulate its nuclear translocation and cellular function. Proc Natl Acad Sci USA 109(21):8149–8154

Sharpe T, Jonsson AL, Rutherford TJ, Daggett V, Fersht AR (2007) The role of the turn in beta-hairpin formation during WW domain folding. Protein Sci 16(10):2233–2239

Smet C, Duckert JF, Wieruszeski JM, Landrieu I, Buee L, Lippens G, Deprez B (2005a) Control of protein–protein interactions: structure-based discovery of low molecular weight inhibitors of the interactions between Pin1 WW domain and phosphopeptides. J Med Chem 48(15):4815–4823

Smet C, Sambo AV, Wieruszeski JM, Leroy A, Landrieu I, Buee L, Lippens G (2004) The peptidyl prolyl cis/trans-isomerase Pin1 recognizes the phospho-Thr212-Pro213 site on Tau. Biochemistry 43(7):2032–2040

Smet C, Wieruszeski JM, Buee L, Landrieu I, Lippens G (2005b) Regulation of Pin1 peptidyl-prolyl cis/trans isomerase activity by its WW binding module on a multi-phosphorylated peptide of Tau protein. FEBS Lett 579(19):4159–4164

Sultana R, Boyd-Kimball D, Poon HF, Cai J, Pierce WM, Klein JB, Markesbery WR, Zhou XZ, Lu KP, Butterfield DA (2006) Oxidative modification and down-regulation of Pin1 in Alzheimer's disease hippocampus: a redox proteomics analysis. Neurobiol Aging 27(7):918–925

Teriete P, Thai K, Choi J, Marassi FM (2009) Effects of PKA phosphorylation on the conformation of the Na, K-ATPase regulatory protein FXYD1. Biochim Biophys Acta 1788(11):2462–2470

Theillet FX, Smet-Nocca C, Liokatis S, Thongwichian R, Kosten J, Yoon MK, Kriwacki RW, Landrieu I, Lippens G, Selenko P (2012) Cell signaling, post-translational protein modifications and NMR spectroscopy. J Biomol NMR 54(3):217–236

Verdecia MA, Bowman ME, Lu KP, Hunter T, Noel JP (2000) Structural basis for phosphoserine-proline recognition by group IV WW domains. Nat Struct Biol 7(8):639–643

Wintjens R, Wieruszeski JM, Drobecq H, Rousselot-Pailley P, Buee L, Lippens G, Landrieu I (2001) 1H NMR study on the binding of Pin1 Trp–Trp domain with phosphothreonine peptides. J Biol Chem 276(27):25150–25156

Wishart DS, Bigam CG, Yao J, Abildgaard F, Dyson HJ, Oldfield E, Markley JL, Sykes BD (1995) 1H, 13C and 15 N chemical shift referencing in biomolecular NMR. J Biomol NMR 6(2):135–140

Wishart DS, Sykes BD (1994) The 13C chemical-shift index: a simple method for the identification of protein secondary structure using 13C chemical-shift data. J Biomol NMR 4(2):171–180

Wittekind M, Reizer J, Deutscher J, Saier MH, Klevit RE (1989) Common structural changes accompany the functional inactivation of HPr by seryl phosphorylation or by serine to aspartate substitution. Biochemistry 28(26):9908–9912

Yaffe MB, Schutkowski M, Shen M, Zhou XZ, Stukenberg PT, Rahfeld JU, Xu J, Kuang J, Kirschner MW, Fischer G, Cantley LC, Lu KP (1997) Sequence-specific and phosphorylation-dependent proline isomerization: a potential mitotic regulatory mechanism. Science 278(5345):1957–1960